第23卷第2期 2004年4月 | 红外与毫米波学报 J. Infrared Millim. Waves | Vol. 23, No.2 April,2004

文章编号:1001-9014(2004)02-0081-05

THEORETICAL ANALYSIS ON GENERATION OF TWIN-PHOTON CONJUGATE CIRCLES IN TYPE-Ⅱ PARAMETRIC DOWN CONVERSION

YU Ke[1,4], ZHANG Yong-Sheng[1,2], ZHU Zi-Qiang[1], LU Wei[3]

(1. Department of Electronic, East China Normal University, Shanghai 200062, China;
2. Department of Computer, Luoyang Technology College, Luoyang 471003, China;
3. State Key Laboratory for infrared Physics, Institute of Technical Physics, Chinese Academy of Sciences, Shanghai 200083, China;
4. School of Physics and Microelectronics, Shandong University, Jinan 250061, China)

Abstract: The equation of the twin photon circles produced in nonlinear optical type-Ⅱ spontaneous parametric down conversion (SPDC) was derived. The change of image of the conjugate circles was analyzed. The interesting features arising from the form of the two-photon state generated in the process were discussed. The geometric optics phenomena of the rings of radiation from the crystal were described. The generation condition of high-efficiency beamlike twin photon was demonstrated.

Key words: type-Ⅱ parametric down conversion; twin photon pairs; phase matching
CLC number: O9431 **Document code**: A

Ⅱ类参量下转换产生孪生光子共轭环的理论分析

郁 可[1,4], 张永胜[1,2], 朱自强[1], 陆 卫[3]

(1. 华东师范大学电子系,上海 200062;
2. 洛阳工业高等专科学校计算机系,河南 洛阳 471003;
3. 中国科学院上海技术物理研究所红外物理国家重点实验室,上海 200083;
4. 山东大学物理与微电子学院,山东 济南 250061)

摘要:推导了非线性光学Ⅱ类参量下转换(SPDC)产生的孪生光子环方程,分析了该共轭环的图象变化,讨论了由双光子态产生的一些有意义的特性,描述了从晶体射出的孪生光子环的几何光学现象,证实了产生高效孪生光子束的条件.

关 键 词:Ⅱ类参量下转换;孪生光子对;相位匹配

Introduction

Experiments with entangled photon pairs, which are created by electron-positron annihilation and in atomic cascade decays, have opened a new field of research due to the entangled photon that allows a distinctive comparison of various concepts of quantum mechanics. Recently, parametric fluorescence (down conversion) in nonlinear optical crystals, as the source of entangled photon pairs,[1,2] was found to lead to a dramatic increase in the count rate. This has enabled a variety of experiments in the foundations of quantum

Received date: 2003-02-24, **revised date**: 2003-12-24 收稿日期:2003-02-24,修回日期:2003-12-24

Foundation Item: The project supported by the National Natural Science Foundation of China (No. 10374027, 69925409) and the Shandong Provincial Natural Science Foundation (No. Y2001G02)

Biography: YU Ke (1963.7-), male, Shandong Jinan, Doctor of East China Normal University, Research area is semiconductor materials and devices, and optics.

mechanics and the realization of new concepts for quantum information[3,4], such as quantum cryptography[5], dense coding[6], and teleportation[7]. However, the experiments and potential application are limited due to the low yield of fluorescence process. One of the main reasons for the small bit rates during the experiments is attributed to the radiation from the crystal photon pairs spreading a wide region. It is difficult to utilize all the photon pairs. In addition, the intensity distribution of the photons selected by an iris is not symmetrical, which causes further difficulties in the experiments.

In this article, we present a theoretical analysis of the image of type-Ⅱ down-converted twin photon conjugate circles. The aim is to understand the characteristic of type-Ⅱ SPDC, optimize collection efficiency, and enhance the available rate of polarization-entangled photon paris.

1 Type-Ⅱ parametric down-conversion

In type-Ⅱ parametric fluorescence, a pump photon with energy $\hbar\omega_p$ is converted in a nonlinear optical crystal into two orthogonally polarized photons, i. e. signal and idler, obeying the laws of energy and momentum conservations. To lead to polarization-entangled photon pairs, the phase-matching condition is satisfied, namely

$$\omega_p = \omega_e + \omega_0,\ \mathbf{k}_p = \mathbf{k}_e + \mathbf{k}_o. \tag{1}$$

Here, ω denotes angular frequency, $\mathbf{k}$ is the wavenumber vector, and subscripts p, o, and e indicate the pump laser light and fluorescence photons with ordinary and extraordinary polarization, respectively.

Although the phase matching equations can be solved numerically, it is more helpful to look for approximate solutions, which lead to a clearer physics picture. The approximation is based on two facts. First, most experiments were carried out for samll angles between the down-converted optical beams direction and the normal direction of output face of the crystal, so that $|\kappa| \ll \omega/c$, κ is the component of the wave vector parallel to the output face of the crystal. Second, the range of frequencies reaching each detector, $\Delta\omega$, is limited, so that $\Delta\omega \ll \omega$.

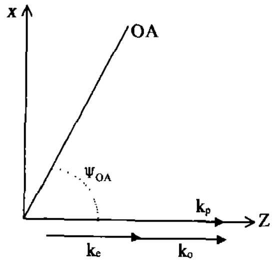

Fig. 1 Collinear perfect phase matching: OA, optic axis of the crystal, lies in the x-z plane
图1 共线完全相位匹配:晶体光轴 OA 在 x-z 平面

A monochromatic plane wave of the pump beam is assumed to travel along the z-axis and the crystal is cut to meet collinear down-conversion perfect phase matching condition (Fig. 1), which are expressed as follows

$$\Omega_e + \Omega_o = \omega_p,\ (K_e + K_o)\hat{e}_z = k_p\hat{e}_z, \tag{2}$$

where

$$K_e = \frac{n_e(\Omega_e, \Psi_{OA})\Omega_e}{c},\ K_o = \frac{n_0(\Omega_o)\Omega_o}{c}. \tag{3}$$

Ψ_{OA} is the angle between the z-axis and optic axis in the x-z plane, namely the phase matching angle. And

$$\frac{1}{n_e(\Omega_e, \Psi_{OA})^2} = \frac{\cos^2\Psi_{OA}}{n_o(\Omega_e)^2} + \frac{\sin^2\Psi_{OA}}{n_e(\Omega_e)^2}, \tag{4}$$

where $n_o(\Omega_e)$ and $n_e(\Omega_e)$ are the principal indices of refraction. In the case of the noncollinear (Fig. 2), we have

$$\omega_e + \omega_o = \omega_p \tag{5}$$

$$\boldsymbol{\kappa}_e + \boldsymbol{\kappa}_o = 0, \tag{6}$$

where, $\boldsymbol{\kappa}_\beta$ ($\beta = e$ or o) is the component of the wave vector parallel to the output face of the crystal. The z component of the two wave vectors for a photon with polarization β is

$$k_{\beta z} = \sqrt{\mathbf{k}_\beta^2 - \boldsymbol{\kappa}_\beta^2}. \tag{7}$$

To calculate phase mismatching $\Delta = k_{pz} - k_{ez} - k_{oz}$, let

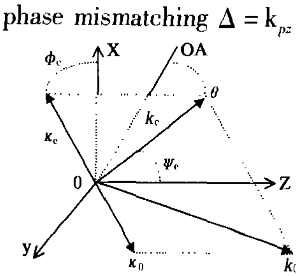

Fig. 2 The e ray and the o ray lie in the same plane which angles ϕ_e with respect to x-z plane. The $\boldsymbol{\kappa}_\beta$ ($\beta = e$ or o) are the transverse components of wave vector, and θ is the angle between $\mathbf{k}_e$ and the optic axis of the crystal
图2 e 光和 o 光在同一平面并与 x-z 面成 ϕ_e 角, $\boldsymbol{\kappa}_\beta$ ($\beta = e$ 或 o) 是波矢的横向分量, θ 是 $\mathbf{k}_e$ 与晶体光轴的夹角

$$\omega_\beta = \Omega_\beta + \nu_\beta, \tag{8}$$

where, $|\nu_\beta| \ll \Omega_\beta$, because the detectors collect output lights in a very narrow band of frequencies in most experiments.

For a typical experiment, the detectors are located in long distance away from the crystal and in a small angle with respect to the pump axis, so that the paraxial approximation is valid. Hence, Eq. (7) can be approximately expressed as series form:

$$k_{\beta z} = k_\beta(\omega) - \frac{\kappa_\beta^2}{2k_\beta(\omega)} + \Lambda . \tag{9}$$

By neglecting the higher than second order terms, and

$$k_\beta(\omega_\beta) = \frac{\omega_\beta n_\beta(\omega_\beta)}{c}, \tag{10}$$

$$k_o = \frac{\omega_o n_o(\omega_o)}{c} = \frac{(\Omega_o + \nu_o) n_o(\omega_o)}{c} \approx K_o + \frac{\nu_0}{u_o}, \tag{11}$$

where u_o is the group velocity of the o-ray evaluated at Ω_o.

$$\frac{1}{u_o} = \frac{d}{d\Omega_o}\frac{\Omega_o n_o(\Omega_o)}{c}. \tag{12}$$

For the o-ray, we have

$$k_{oz} = \sqrt{k_o^2 - \kappa_o^2} \approx k_o - \frac{\kappa_o^2}{2K_o} \approx K_o + \frac{\nu_o}{u_o} - \frac{\kappa_o^2}{2K_o}. \tag{13}$$

For the e-ray, the index of refraction varies with the direction of wave vector. Using ω_e and $\boldsymbol{\kappa}_e$ as independent variables and referring to Fig. 2, we obtain

$$k_{ez} = \sqrt{k_e^2(\omega_e, \theta) - \kappa_e^2} \approx K_e + \frac{\nu_e}{u_e} + \frac{\partial k_e}{\partial \boldsymbol{\kappa}_e} \cdot \boldsymbol{\kappa}_e - \frac{\kappa_e^2}{2K_e}, \tag{14}$$

$$\frac{1}{u_e} = \frac{\partial}{\partial \Omega_e}\left(\frac{\Omega_e n_e(\Omega_e, \Psi_{OA})}{c}\right), \tag{15}$$

where u_e is the group velocity of e-ray at Ω_e. From Eq. (10), we obtain

$$\frac{\partial k_e}{\partial \boldsymbol{\kappa}_e} = \frac{\omega_e}{c}\frac{\partial n_e(\omega_e, \theta)}{\partial \boldsymbol{\kappa}_e} = \frac{\omega_e}{c}\frac{\partial \theta}{\partial \boldsymbol{\kappa}_e}\frac{\partial n_e(\omega_e, \theta)}{\partial \theta}. \tag{16}$$

Considering the projection of k_e on the optic axis, we get

$$k_e \cos\theta = k_{ez}\cos\Psi_{OA} + \kappa_{ex}\cos\left(\frac{\pi}{2} - \Psi_{OA}\right). \tag{17}$$

Differentiating both sides of Eq. (17) with respect to $\boldsymbol{\kappa}_e$, we obtain

$$\frac{\partial k_e}{\partial \boldsymbol{\kappa}_e}\cos\theta - k_e \sin\theta \frac{\partial \theta}{\partial \boldsymbol{\kappa}_e} = \frac{\partial k_{ez}}{\partial \boldsymbol{\kappa}_e}\cos\Psi_{OA} + \frac{\partial \kappa_{ex}}{\partial \boldsymbol{\kappa}_e}\sin\Psi_{OA}$$

$$= \left(\frac{k_e}{k_{ez}}\frac{\partial k_e}{\partial \boldsymbol{\kappa}_e} - \frac{\boldsymbol{\kappa}_e}{k_{ez}}\right)\cos\Psi_{OA} + \frac{\partial \kappa_{ex}}{\partial \boldsymbol{\kappa}_e}\sin\Psi_{OA}. \tag{18}$$

Substituting Eq. (16) into Eq. (18), we obtain for $\boldsymbol{\kappa}_e = 0$

$$\delta_{rx}\sin\Psi_{OA} = k_e\left[N\left(\cos\theta - \frac{k_e}{k_{ez}}\cos\Psi_{OA}\right) - \sin\theta\right]\frac{\partial \theta}{\partial \kappa_{er}}, \tag{19}$$

here

$$N = \frac{\partial ln[n_e(\Omega_e, \Psi_{OA})]}{\partial \Psi_{OA}} = \frac{1}{2}n_e^2(\Omega_e, \Psi_{OA})\left(\frac{1}{n_o^2(\Omega_e)} - \frac{1}{n_e^2(\Omega_e)}\right)\sin(2\Psi_{OA}). \tag{20}$$

In Eq. (19) $r = x$ or y, for $\boldsymbol{\kappa}_e = 0$, $\omega_e \approx \Omega_e$, $\theta \approx \Psi_{OA}$, $k_e \approx k_{ez} \approx K_e$, Eq. (19) reduces to

$$\frac{\partial \theta}{\partial \kappa_{er}} = -\delta_{rx}\frac{1}{K_e}. \tag{21}$$

Substituting Eq. (21) into Eq. (16), we get

$$\frac{\partial k_e}{\partial \boldsymbol{\kappa}_e} \cdot \boldsymbol{\kappa}_e = \frac{\omega_e}{c}\frac{\partial n_e(\omega_e, \theta)}{\partial \theta}\frac{\partial \theta}{\partial \boldsymbol{\kappa}_e} \cdot \boldsymbol{\kappa}_e$$

$$= k_e N\left(\frac{\partial \theta}{\partial \kappa_{ex}}\kappa_{ex} + \frac{\partial \theta}{\partial \kappa_{ey}}\kappa_{ey}\right)$$

$$= -k_e N \cdot \frac{\kappa_{ex}}{\kappa_e} = -N\kappa_{ex}, \tag{22}$$

$$k_{ez} = K_e + \frac{\nu_e}{u_e} - \kappa_{ex}N - \frac{\kappa_e^2}{2K_e}, \tag{23}$$

From Eq. (2), (5) and (8), $\nu_o = -\nu_e \equiv -\nu$. Using Eq. (6), (13) and (23), we obtain

$$\begin{aligned}\Delta &= k_{pz} - k_{ez} - k_{oz} = k_p - k_{ez} - k_{oz} \\ &= K_e + K_o - k_{ez} - k_{oz} \\ &= \nu D - \frac{N^2\bar{K}}{4} + \frac{1}{\bar{K}}\left(\boldsymbol{\kappa}_e + \frac{N\bar{K}}{2}\hat{\mathbf{e}}_x\right)^2,\end{aligned} \tag{24}$$

where

$$\frac{1}{\bar{K}} = \frac{1}{2}\left(\frac{1}{K_o} + \frac{1}{K_e}\right), \quad D = \frac{1}{u_o} - \frac{1}{u_e}. \tag{25}$$

For perfect phase matching condition $\Delta = 0$, and a

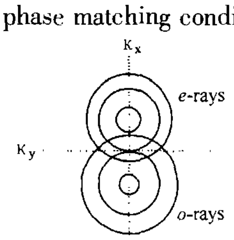

Fig. 3　Schematic of two sets of conjugate rings for type-Ⅱ parametric down-conversion (N < 0). The circle corresponding to $\omega_e = \omega_o$ are tangent to the κ_y axis.

图 3　两组Ⅱ类参量下转换共轭环的示意图(N < 0). 当 $\omega_e = \omega_o$ 时, 两圆环切于 κ_y 轴

fixed ν, Eq. (24) gives the circle equation for $\boldsymbol{\kappa}_e$ in the κ plane. The center of the circle is at $-(\overline{NK}/2)\hat{\mathbf{e}}_x$, and the radius equals to $\sqrt{N^2K^2/4-\nu DK}$. When $\nu=0$, the circle is tangent at the origin to the κ_y axis (Fig. 3). The *o-rays* make a complementary circle at $-\boldsymbol{\kappa}_e$.

2 Results and discussion

For a negative birefringent crystal, $D>0, N<0$. For $\nu<0$, as indicated in Eq. (8), ω_e decreases and ω_o increases when $|\nu|$ increasing, which leads to an increase in the radii of the circle and overlap of the *e-ray* and *o-ray* circles[8]. This situation can be realized by increasing Ψ_{OA}[9]. A pair of conjugate circle intersects at points of the κ_y axis. The distance between intersection points and the origin in the κ plane is $\kappa=\sqrt{-\nu|D|\overline{K}}$. The center of the circle pair lies in the plane of the optic axis and the pump wave vector. The *e*-ray lies in the half plane of positive κ_x for negative $N(n_e(\omega)<n_o(\omega))$.

For $\nu>0$, increasing ν results in an increase of ω_e and the decrease of ω_o. The circle pair become small and separates each other. This situation can be realized by adjusting the crystal and reducing Ψ_{OA}.

Outside the crystal, the angle between the wave vector and the *z*-axis, θ_r, is given by $\sin\theta_r=c\kappa_r/\omega_r$, here $r=o$ or e. This means that the conjugate circles outside the crystal have different radii when $\omega_e\neq\omega_o$.

For a given crystal type, the curves of pump wavelength and Ψ_{OA} which are plots of the signal (*e*-ray) and idler (*o*-ray) wavelengths λ versus the crystal emission angles α, can be approximately obtained from Eq. (1), Snell's law and a lot of related parameters. For BBO crystal, the wavelength of the pump beam is

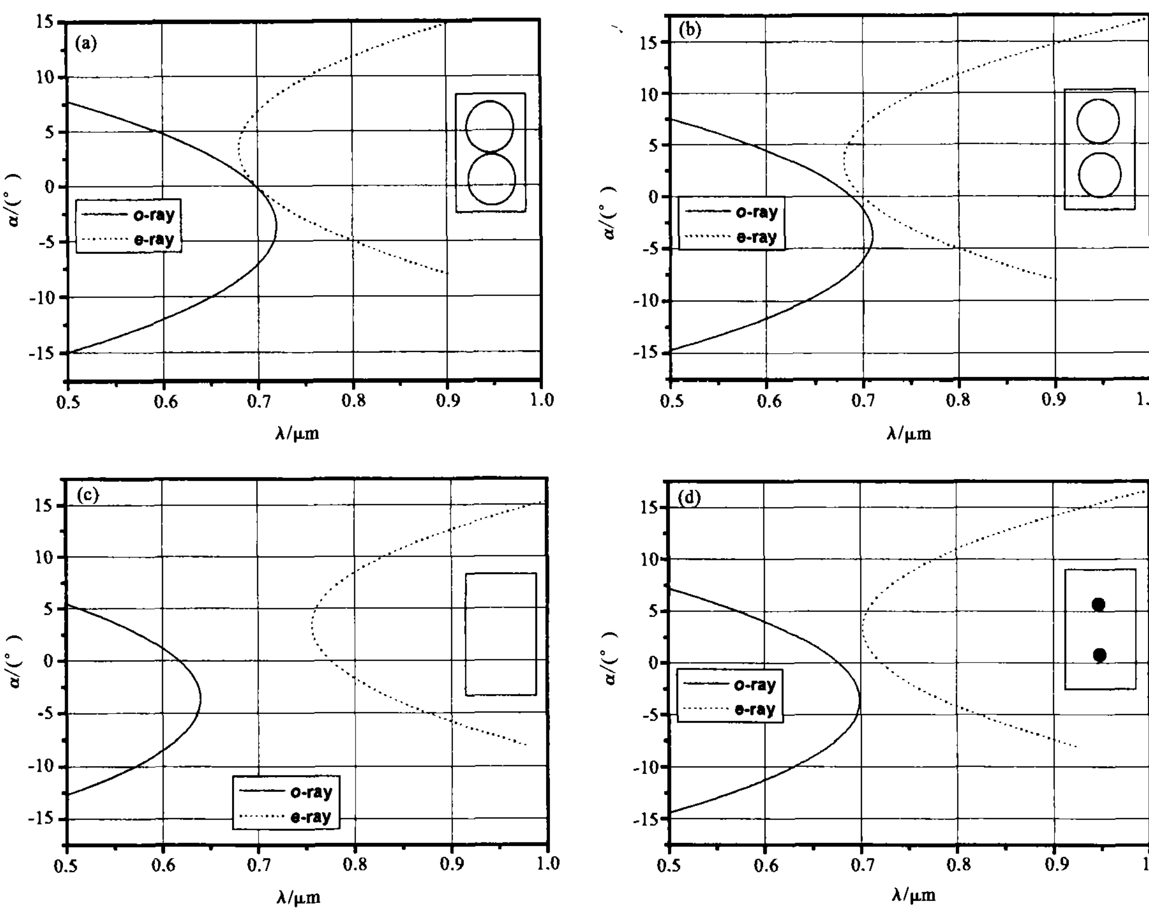

Fig. 4 The tuning curves in which the dashed curve indicates the signal beam, and the solid curve indicates the idler beam. The insets are images of the parametric fluorescence: (a) collinear condition, $\Psi_{OA}\approx49°$ (b) $\Psi_{OA}\approx48°$ (c) $\Psi_{OA}\approx45.6°$ (d) condition for twin-beam generation, $\Psi_{OA}\approx47°$

图4 调谐曲线,长划线表示信号光束,实线表示休闲光束,插图是参量荧光像:(a)共线条件,$\Psi_{OA}\approx49°$ (b)$\Psi_{OA}\approx48°$ (c)$\Psi_{OA}\approx45.6°$ (d)$\Psi_{OA}\approx47°$

351nm. The curves of various cases are shown in Fig. 4, where the optic axis, $\mathbf{k}_p$, $\mathbf{k}_e$, $\mathbf{k}_o$ all lie in the same plane.

Figure 4 (a) shows the case of collinear condition, $\Psi_{OA} \approx 49°$, in which the signal and idler photon travel collinearly with the degenerate wavelength of 702nm. The inset shows an image of the emitted twin photons at 702nm when one is facing the crystal to observe. These twin photons are emitted into two cones that touch in the pump-beam direction. This condition has been widely used in experiment. However, here only a small portion of the whole ensemble of emitted photons is utilized.

When Ψ_{OA} is decreased, these two curves separate each other; the circles shrink and move away gradually [Fig. 4(b)]. When $\Psi_{OA} > 47°$, the circles vanish and no photons are emitted, which is shown in Fig. 4(c). When Ψ_{OA} is about 47°, the two curves are tangent to the line at the wavelength of 702nm. Twin photons will be emitted into two small spots, and beamlike twin photons are generated [Fig. 4(d)]. In this case, high-efficiency entangled photon pair collection for type-Ⅱ parametric fluorescence can be realized and a high single-cuton rate and a high coincidence-count rate per unit of pump power can be observed in the experiment.

3 Conclusion

In summary, we have presented a theoretical analysis on the twin photon pairs generated in type-Ⅱ SPDC. A detailed discussion of phase matching has allowed us to describe the physical phenomena of the beautiful colored rings that can be photographed emerging from the down-conversion crystal[8]. The generation condition of beamlike twin photon has been demonstrated. We expect that the results will have potential application in experiments of high-efficiency collection entangled photon pairs created in a type-Ⅱ SPDC, so that strong sources for polarization entangled photon will be produced.

REFERENCES

[1] Hong C K, Mandel L. Theory of parametric frequency down conversion of light [J]. *Phys. Rev. A.*, 1985, **31** (4): 2409—2418

[2] Rarity J G, Tapster P R. Experimental violation of Bell's inequality based on phase and momentum [J]. *Phys. Rev. Lett.*, 1990, **64**(21): 2495—2498

[3] Bouwmeester D, Pan J W, Mattle K, *et al.* Experimental quantum teleportation [J]. *Nature*, 1997, **390**: 575—579

[4] Bouwmeester D, Pan J W, Daniell M, *et al.* Observation of three-photon Greenberger-Horne-Zeilinger entanglement [J]. *Phys. Rev. Lett.*, 1999, **82**(7): 1345—1349

[5] Ekert A K. Quantum cryptography based on Bell's theorem [J]. *Phys. Rev. Lett.*, 1991, **67**(6): 661—663

[6] Bennett C H, Wiesner S J. Communication via one-and two-particle operators on Einstein-Podolsky-Rosen states [J]. *Phys. Rev. Lett.*, 1992, **69**(20): 2881—2884

[7] Bennett C H, Brassard G, Crepeau C, *et al.* Teleporting an unknown quantum state via Dual classical and Einstein-Podolsky-Rosen channels [J]. *Phys. Rev. Lett.*, 1993, **70** (13): 1895—1899

[8] Kwiat P G, Mattle K, Weinfurter H, *et al.* New high-intensity source of polarization-entangled photon pairs [J]. *Phys. Rev. Lett.*, 1995, **75**(24): 4337—4341

[9] Sutherland R L, *Handbook of Nonlinear Optics* [M]. New York: Marcel Dekker, Inc., 1996: 143—151